Semiconductor Physics, Quantum Electronics & Optoelectronics, 2016. V. 19, N 4. P. 371-376.
doi: https://doi.org/10.15407/spqeo19.04.371

PACS 42.70.Gi, 68.65.Ac, 81.15.Fg

Compositional studies of optical parameters in $(Ag_3AsS_3)_x(As_2S_3)_{1-x}$ (x = 0.3; 0.6; 0.9) thin films

I.P. Studenyak[1], M. Kranjčec[2], M.M. Kutsyk[1], Yu.O. Pal[1], Yu.Yu. Neimet[1], V.Yu. Izai[1], I.I. Makauz[1], C. Cserhati[3], S. Kökényesi[3]
[1]*Faculty of Physics, Uzhhorod National University, 3, Narodna Sq., 88000 Uzhhorod, Ukraine*
[2]*Department of Civil Engineering, University North, 33, J. Križanića St., 642000 Varaždin, Croatia*
[3]*Faculty of Science and Technology, University of Debrecen, 18/a Bem Sq., 4026 Debrecen, Hungary*
E-mail: studenyak@dr.com

Abstract. $(Ag_3AsS_3)_x(As_2S_3)_{1-x}$ (x = 0.3; 0.6; 0.9) thin films were deposited onto a silica substrate by rapid thermal evaporation. The amount of Ag-rich crystalline phase precipitates on the surfaces of the films increases with Ag_3AsS_3 content. It has been shown that the absorption edge spectra are described by the Urbach rule. The temperature behaviour of absorption spectra was studied, the temperature dependences of energy position of absorption edge and Urbach energy were also investigated. The influence of compositional disordering due to Ag_3AsS_3 introduction into As_2S_3 on the optical parameters of $(Ag_3AsS_3)_x(As_2S_3)_{1-x}$ thin films were analyzsed. The spectral, temperature and compositional behaviour of refractive index for $(Ag_3AsS_3)_x(As_2S_3)_{1-x}$ thin films were studied.

Keywords: thin film, optical absorption, Urbach energy, refractive index, compositional dependence, electron-phonon interaction.

Manuscript received 03.06.16; revised version received 18.08.16; accepted for publication 16.11.16; published online 05.12.16.

1. Introduction

Glasses and composites of Ag–As–S system are promising materials for creation of solid electrolytes, electrochemical sensors, electrochromic displays *etc*. [1, 2]. It should be noted that, in comparison with crystalline solid electrolytes, chalcogenide glasses are more technological, simple and lower-cost in production. Recently, we have reported about the structure [3], electrical conductivity [4], and optical absorption [5] in superionic Ag_3AsS_3–As_2S_3 glasses and composites. X-ray studies have manifested the glasses of Ag–As–S system to get separated after adding the proustite Ag_3AsS_3 crystal to the base As_2S_3 glass [4]. It should be noted that one can distinguish three different structural states in the whole compositional range of the $(Ag_3AsS_3)_x(As_2S_3)_{1-x}$ system: glassy state for x = 0…0.4, composite state with crystalline smithite $AgAsS_2$ inclusions for $0.4 < x \le 0.6$, and a composite state with crystalline smithite $AgAsS_2$ and proustite Ag_3AsS_3 inclusions for $0.6 < x < 1$ [6].

Thin films in above mentioned system were mostly prepared by a deposition onto the substrates using

Semiconductor Physics, Quantum Electronics & Optoelectronics, 2016. V. 19, N 4. P. 371-376.
doi: https://doi.org/10.15407/spqeo19.04.371

vacuum coating techniques, *i.e*. thermal evaporation accompanied by a thermal or photo-induced dissolution of silver in As_2S_3 matrix [7, 8]. In Ref. [9], we have presented the results of deposition of $(Ag_3AsS_3)_{0.6}(As_2S_3)_{0.4}$ thin films by the rapid thermal evaporation in vacuum. SEM and AFM imaging of the thin films revealed numerous micrometer-sized cones on their surfaces. It was shown that annealing and illumination lead to the increase of the energy position of absorption edge, and to a decrease of the refractive index. The influence of the deposition technology on structural and optical properties of $(Ag_3AsS_3)_{0.6}(As_2S_3)_{0.4}$ thin films was studied in Ref. [10]. In Ref. [11], we have reported on the temperature behavior of optical absorption edge and refractive index in $(Ag_3AsS_3)_{0.6}(As_2S_3)_{0.4}$ thin films, while the photo-induced changes were investigated in Ref. [12].

This paper is devoted to deposition, investigation of optical transmission spectra, analyses of optical absorption edge and refractive index dispersion as well as the compositional studies of optical parameters in $(Ag_3AsS_3)_x(As_2S_3)_{1-x}$ thin films with x = 0.3; 0.6; 0.9.

2. Experimental

Synthesis of $(Ag_3AsS_3)_x(As_2S_3)_{1-x}$ glasses and composites with x = 0.3; 0.6; 0.9 was carried out at the temperatures 820…840 K for 24 h with subsequent melt homogenization for 72 h. Thin films were prepared by rapid thermal evaporation from the corresponding material at near 1350 °C in vacuum ($3\cdot10^{-3}$ Pa) using the VU-2M setup. The material was initially placed in a tantalum evaporator perforated for preventing the material falling out on a glass substrate kept at room temperature. The film thickness was measured using an Ambios XP-1 profile meter.

Structural properties of the films under investigation were studied using scanning electron microscopy (Hitachi S-4300). It is shown that increase of Ag_3AsS_3 in thin films leads to appearance of cones and nano-size inclusions on the top of as-evaporated thin films surface with chemical composition different from that of the main film (Fig. 1). The number of cones on the surface of the investigated thin films increased with increase of Ag_3AsS_3 content.

The chemical composition of as-deposited thin films was determined using EDX technique. Thus, the films deposited from $(Ag_3AsS_3)_{0.3}(As_2S_3)_{0.7}$ glass were Ag- and As-enriched and had a deficiency of sulphur ($Ag_{1.5}As_{2.2}S_{1.9}$) in comparison with the initial bulk material ($Ag_{0.9}As_{1.7}S_3$); the films deposited from $(Ag_3AsS_3)_{0.6}(As_2S_3)_{0.4}$ composite had the Ag content most close to initial bulk material ($Ag_{1.8}As_{1.4}S_3$), since it is As-enriched and has a deficiency of sulphur ($Ag_{1.8}As_2S_{2.4}$); the films deposited from $(Ag_3AsS_3)_{0.9}(As_2S_3)_{0.1}$ composite were As-enriched and had a deficiency of silver and sulphur ($Ag_{1.7}As_{3.2}S_{2.6}$) in comparison with the initial bulk material ($Ag_{2.7}As_{1.1}S_3$).

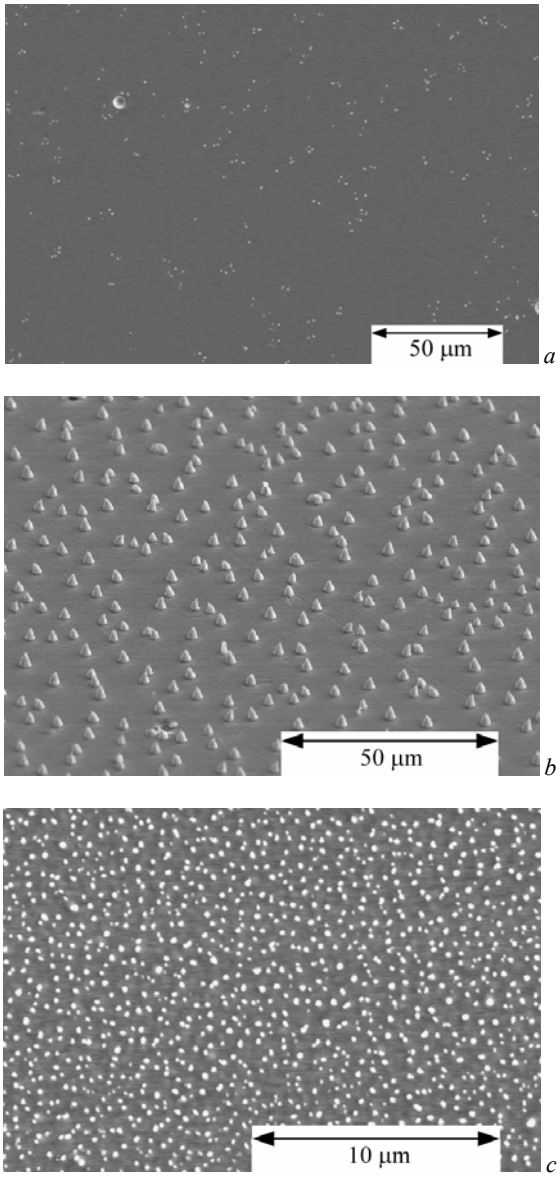

Fig. 1. SEM images of thermally evaporated $(Ag_3AsS_3)_{0.3}(As_2S_3)_{0.7}$ (a), $(Ag_3AsS_3)_{0.6}(As_2S_3)_{0.4}$ (b) and $(Ag_3AsS_3)_{0.9}(As_2S_3)_{0.1}$ (c) thin films.

Optical transmission spectra were studied within the range of temperatures 77 to 300 K by using the MDR-3 grating monochromator and UTREX-type cryostat. From the temperature studies of interference transmission spectra, the spectral dependences of the absorption coefficient as well as dispersion dependences of the refractive index were derived [13].

3. Results and discussion

Interferential transmission spectra of $(Ag_3AsS_3)_x(As_2S_3)_{1-x}$ thin films are the same for all the investigated films. Fig. 2 presents, as an example, the interferential transmission spectra of

$(Ag_3AsS_3)_{0.9}(As_2S_3)_{0.1}$ thin film at various temperatures within the range 77…300 K. With temperature increase, the longwave shift of high-energy parts of transmission spectra and transmittance decrease at interferential maxima are observed. Based on the interferential transmission spectra, the spectral dependences of absorption coefficient and refractive index were obtained. It has been shown (Fig. 3) that the optical absorption edge in the region of its exponential behaviour is described by the Urbach rule [14]:

$$\alpha(h\nu,T)=\alpha_0\cdot\exp\left[\frac{\sigma(h\nu-E_0)}{kT}\right]= \\ =\alpha_0\cdot\exp\left[\frac{h\nu-E_0}{E_U(T)}\right], \quad (1)$$

where E_U is the Urbach energy (a reciprocal of the absorption edge slope $E_U^{-1}=\Delta(\ln\alpha)/\Delta(h\nu)$), σ is the absorption edge steepness parameter, α_0 and E_0 are the convergence point coordinates of the Urbach bundle. The coordinates of the Urbach bundle convergence point α_0 and E_0 for the $(Ag_3AsS_3)_x(As_2S_3)_{1-x}$ thin films are given in Table. It should be noted that α_0 and E_0 values for the films under investigation increase in comparison with those in the As_2S_3 thin film.

Table. Parameters of the Urbach absorption edge and EPI for As_2S_3, $(Ag_3AsS_3)_{0.3}(As_2S_3)_{0.7}$, $(Ag_3AsS_3)_{0.6}(As_2S_3)_{0.4}$ and $(Ag_3AsS_3)_{0.9}(As_2S_3)_{0.1}$ thin films.

Film	As_2S_3	$(Ag_3AsS_3)_{0.3}(As_2S_3)_{0.7}$	$(Ag_3AsS_3)_{0.6}(As_2S_3)_{0.4}$	$(Ag_3AsS_3)_{0.9}(As_2S_3)_{0.1}$
E_g^α (eV)	2.746	2.681	2.086	2.382
E_U (meV)	109.4	231	403	264
α_0 (cm^{-1})	$5.34\cdot10^4$	$9.6\cdot10^4$	$3.2\cdot10^5$	$6.9\cdot10^5$
E_0 (eV)	2.754	2.831	2.828	3.076
σ_0	0.264	0.155	0.106	0.171
$\hbar\omega_p$ (meV)	30.2	59.6	77.7	84.2
θ_E (K)	351	249	301	227
$(E_U)_0$ (meV)	57.2	181	360	238
$(E_U)_1$ (meV)	114.7	64.5	74.2	28.9
$E_g^\alpha(0)$ (eV)	2.529	2.714	2.165	2.449
S_g^α	15.1	1.95	5.27	3.89
n	2.42	3.58	3.08	2.54

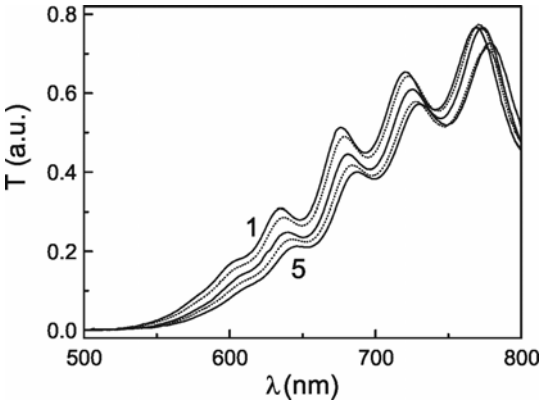

Fig. 2. Optical transmission spectra of $(Ag_3AsS_3)_{0.9}(As_2S_3)_{0.1}$ thin film at various temperatures: 77 (*1*), 150 (*2*), 200 (*3*), 250 (*4*), and 300 K (*5*).

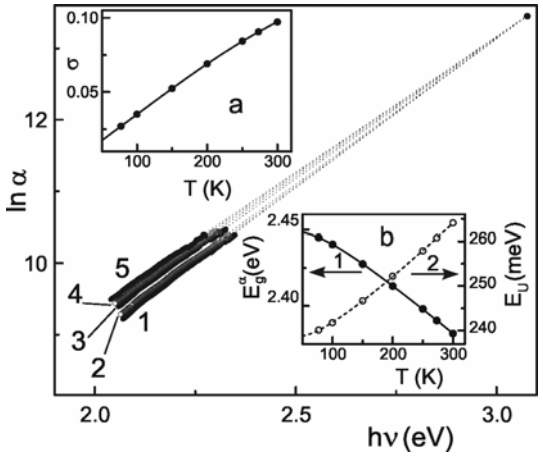

Fig. 3. Spectral dependences of the absorption coefficient of $(Ag_3AsS_3)_{0.9}(As_2S_3)_{0.1}$ thin film at various temperatures: 77 (*1*), 150 (*2*), 200 (*3*), 250 (*4*) and 300 K (*5*). The inserts show the temperature dependence of the steepness parameter σ (a) and temperature dependences of the absorption edge energy position E_g^α ($\alpha = 5\cdot10^4$ cm^{-1}) (*1*) and Urbach energy E_U (*2*) for $(Ag_3AsS_3)_{0.9}(As_2S_3)_{0.1}$ thin film (b). The size of experimental point symbols exceeds the error bars which are $\pm5\cdot10^{-4}$ eV for E_g^α and $\pm2\cdot10^{-4}$ eV for E_U.

The temperature behaviour of the Urbach absorption edge in $(Ag_3AsS_3)_x(As_2S_3)_{1-x}$ films is explained by electron-phonon interaction (EPI) which is strong in the films under investigation. The EPI parameters are obtained from the temperature dependence of absorption edge steepness parameter (Fig. 3) using the Mahr formula [15]:

$$\sigma(T)=\sigma_0\cdot\left(\frac{2kT}{\hbar\omega_p}\right)\cdot\tanh\left(\frac{\hbar\omega_p}{2kT}\right), \quad (2)$$

where $\hbar\omega_p$ is the effective phonon energy in the one-oscillator model describing the electron-phonon

interaction (EPI), and σ_0 is a parameter related to the EPI constant g as $\sigma_0 = (2/3)g^{-1}$ (parameters $\hbar\omega_p$ and σ_0 are given in Table). For the $(Ag_3AsS_3)_{0.9}(As_2S_3)_{0.1}$ thin film, $\sigma_0 < 1$ that is the evidence for the strong EPI [16]. Besides, in $(Ag_3AsS_3)_x(As_2S_3)_{1-x}$ thin films, compared to the As_2S_3 thin film, EPI is substantially enhanced (this corresponds to a decrease of the σ_0 parameter), and the energy $\hbar\omega_p$ of the effective phonon taking part in absorption edge formation increases (Table).

Temperature dependences of the energy position of the exponential absorption edge E_g^α (E_g^α values taken at a fixed absorption coefficient value $\alpha = 5\cdot10^4$ cm^{-1}) and Urbach energy E_U (Fig. 3) are well described within the framework of Einstein model [17, 18]:

$$E_g^\alpha(T) = E_g^\alpha(0) - S_g^\alpha k\,\theta_E\left[\frac{1}{\exp(\theta_E/T)-1}\right], \quad (3)$$

$$(E_U) = (E_U)_0 + (E_U)_1\left[\frac{1}{\exp(\theta_E/T)-1}\right], \quad (4)$$

where $E_g^\alpha(0)$ and S_g^α are the energy position of absorption edge at 0 K and a dimensionless constant, respectively; θ_E is the Einstein temperature corresponding to the average frequency of phonon excitations of a system of non-coupled oscillators, $(E_U)_0$ and $(E_U)_1$ are the constants. The obtained $E_g^\alpha(0)$, S_g^α, θ_E, $(E_U)_0$, and $(E_U)_1$ parameters for the thin films under investigation are given in Table and the temperature dependences of E_g^α and E_U for the $(Ag_3AsS_3)_x(As_2S_3)_{1-x}$ thin films calculated using Eqs. (3) and (4), are shown in Fig. 3 by solid and dashed lines, respectively.

The broadening and smearing of the absorption edge spectra in thin films under investigation are observed in comparison with the bulk composite. Thus, the Urbach energy E_U in $(Ag_3AsS_3)_{0.6}(As_2S_3)_{0.4}$ thin film is more than five times higher than that in the bulk composite [5]. It was shown that temperature, structural and compositional disordering affect Urbach absorption edge shape, *i.e.* the Urbach energy E_U is described by the equation [19]

$$E_U = (E_U)_T + (E_U)_X + (E_U)_C = (E_U)_T + (E_U)_{X+C}, \quad (5)$$

where $(E_U)_T$, $(E_U)_X$ and $(E_U)_C$ are contributions of temperature, structural and compositional disordering to E_U, respectively. It should be noted that the first term in the right-hand side of Eq. (4) represents the sum of structural and compositional disordering, and the second one represents temperature disordering. For separation of contribution of different types of disordering into the Urbach energy, we used the procedure developed in Ref. [20].

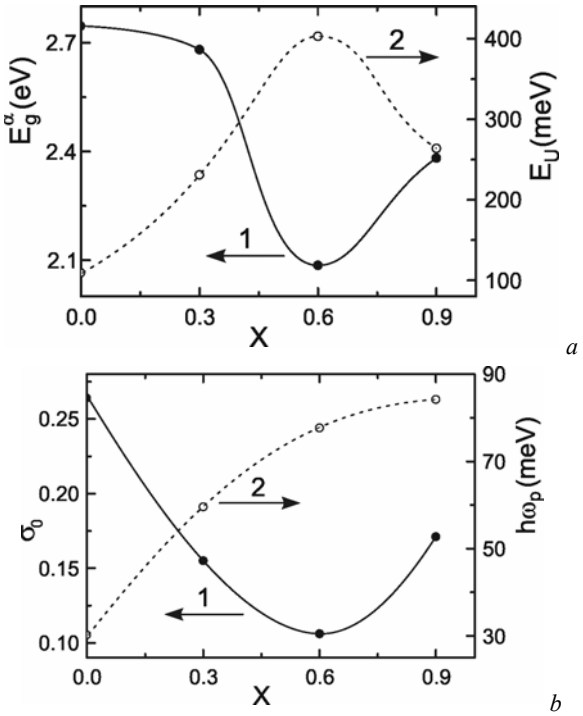

Fig. 4. (a) Compositional dependences of the absorption edge energy position E_g^α ($\alpha = 5\cdot10^4$ cm^{-1}) (1) and Urbach energy E_U (2) of $(Ag_3AsS_3)_x(As_2S_3)_{1-x}$ thin films at 300 K. (b) Compositional dependences of σ_0 constant and effective phonon energy $\hbar\omega_p$ values of $(Ag_3AsS_3)_x(As_2S_3)_{1-x}$ thin films. The size of the experimental point symbols exceeds the error bars that are $\pm5\cdot10^{-4}$ eV for E_g^α, $\pm2\cdot10^{-4}$ eV for E_U and $\hbar\omega_p$, $\pm5\cdot10^{-3}$ for σ_0.

Finally, it should be noted that the shape and temperature behavior of optical absorption edge, dispersion and temperature dependences of the refractive index for the different chemical compositions of $(Ag_3AsS_3)_x(As_2S_3)_{1-x}$ thin films are similar to $(Ag_3AsS_3)_{0.9}(As_2S_3)_{0.1}$ thin film dependences given as an example.

The compositional studies show that with the increase of the content of Ag_3AsS_3 in $(Ag_3AsS_3)_x(As_2S_3)_{1-x}$ thin films the nonlinear decrease of E_g^α value with its minimum at $x = 0.6$ and the nonlinear increase of Urbach energy with its maximum at $x = 0.6$ were revealed (Fig. 4a). Besides, the nonlinear decrease of σ_0 constant with its minimum at $x = 0.6$, which is the evidence of EPI enhancement, and monotonical nonlinear increase of $\hbar\omega_p$ energy with increase of Ag_3AsS_3 content are observed in $(Ag_3AsS_3)_x(As_2S_3)_{1-x}$ thin films (Fig. 4b). The contribution of different types of disordering was estimated from Urbach energy temperature dependences in accord with Eq. (4). The nonlinear behavior of Urbach energy and the sum of contribution of structural and compositional disordering (Fig. 5) is explained by the influence of compositional

disordering. It reflects by the compositional dependence of absolute value of $(E_U)_{X+C}$ that has the specific maximum at $x = 0.6$ due to the influence of compositional disordering (Fig. 5). Also, good correlation between σ_0, $\hbar\omega_p$ and $(E_U)_{X+C}$ compositional dependences is observed.

The slight dispersion of the refractive index is observed in the transparency region, while it increases when approaching to the optical absorption edge region (Fig. 6). With increasing the temperature, the nonlinear growth of the refractive index in $(Ag_3AsS_3)_{0.9}(As_2S_3)_{0.1}$ thin film is revealed. The nonlinear compositional dependence of the refractive index value at 1 μm with its maximum at $x = 0.3$ (Fig. 6) can be associated with the maximal optical density of still homogenous film with a high content of Ag_3AsS_3. The further increase of Ag_3AsS_3 content leads to appearance of phase precipitates and formation of a heterophase system.

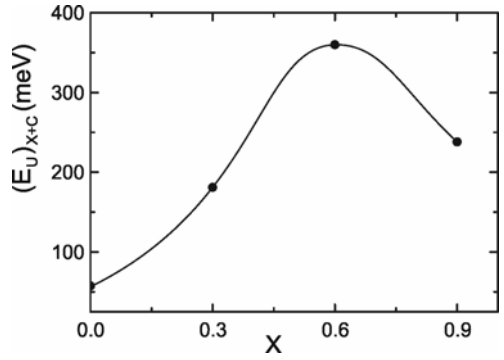

Fig. 5. Compositional dependences of absolute values of static structural disordering contribution and compositional disordering contribution to the Urbach energy for $(Ag_3AsS_3)_x(As_2S_3)_{1-x}$ thin films.

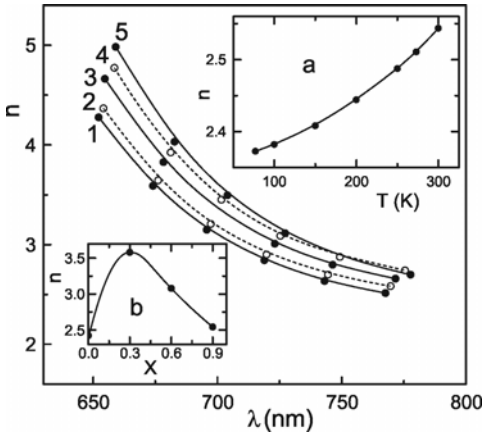

Fig. 6. Refractive index dispersions of $(Ag_3AsS_3)_{0.9}(As_2S_3)_{0.1}$ thin film at various temperatures: 77 (*1*), 150 (*2*), 200 (*3*), 250 (*4*), and 300 K (*5*). The inserts show the temperature dependence of refractive index (a) and compositional dependence of it (b) for $(Ag_3AsS_3)_x(As_2S_3)_{1-x}$ thin films. The size of the experimental point symbols exceeds the error bars that are $\pm 1 \cdot 10^{-4}$ for *n*.

Conclusions

$(Ag_3AsS_3)_x(As_2S_3)_{1-x}$ thin films were deposited onto a silica substrate by rapid thermal evaporation. SEM imaging of the thin films indicated formation of numerous micrometer- and submicrometer-sized Ag-containing phase precipitates on their surfaces with increase of Ag_3AsS_3 content. The spectral dependences of the absorption coefficient as well as dispersion dependences of the refractive index were derived from the spectrometric studies of interferential transmission spectra. In the range of the exponential behaviour of the optical absorption edge, the energy position of exponential absorption edge E_g^{α} and Urbach energy E_U in $(Ag_3AsS_3)_x(As_2S_3)_{1-x}$ thin films were determined. Temperature variation of the transmission spectra as well as the temperature behaviour of the absorption edge spectra within the range of its exponential behaviour were studied. A typical Urbach bundle has been observed, temperature dependences of the absorption edge energy position and the Urbach energy were obtained. The influence of different types of disordering on the Urbach tail was studied and analysis of compositional dependences of the Urbach absorption edge parameters for $(Ag_3AsS_3)_x(As_2S_3)_{1-x}$ thin films was performed.

References

1. A. Pradel, N. Kuwata, M. Ribes, Ion transport and structure in chalcogenide glasses // *J. Phys.: Condens. Matter*, **15**, p. 1561-1571 (2003).
2. E. Bychkov, D.L. Price, C.J. Benmore, A.C. Hannon, Ion transport regimes in chalcogenide and chalcohalide glasses: from the host to the cation-related network connectivity // *Solid State Ionics*, **154-155**, p. 349-359 (2002).
3. I. Studenyak, Yu. Neimet, C. Cserhati, S. Kökényesi, E. Kazakevičius, T. Šalkus, A. Kežionis, A. Orliukas, Structural and electrical investigations of $(Ag_3AsS_3)_x(As_2S_3)_{1-x}$ superionic glasses // *Cent. Eur. J. Phys.* **10**, p. 206-209 (2012).
4. I.P. Studenyak, Yu.Yu. Neimet, M. Kranjčec, A.M. Solomon, A.F. Orliukas, A. Kežionis, E. Kazakevičius, T. Šalkus, Electrical conductivity studies in $(Ag_3AsS_3)_x(As_2S_3)_{1-x}$ superionic glasses and composites // *J. Appl. Phys*. **115**, p. 033702-1−033702-5 (2014).
5. I.P. Studenyak, M. Kranjcec, Yu.Yu. Neimet, M.M. Pop, Optical absorption edge in $(Ag_3AsS_3)_x(As_2S_3)_{1-x}$ superionic glasses // *Semiconductor Physics, Quantum Electronics & Optoelectronics*, **15**, p. 147-151 (2012).
6. I.P. Studenyak, Yu.Yu. Neimet, A.F. Orliukas, A. Kežionis, E. Kazakevičius, T. Šalkus, Dielectric permittivity in $(Ag_3AsS_3)_x(As_2S_3)_{1-x}$ superionic glasses and composites // *Semiconductor Physics, Quantum Electronics & Optoelectronics*, **17**, p. 174-178 (2014).

7. T. Wagner, V. Perina, A. Mackov, E. Rauhala, A. Seppala, Mir. Vlcek, S.O. Kasap, Mil. Vlcek, M. Frumar, The tailoring of the composition of Ag–As–S amorphous films using photo-induced solid state reaction between Ag and $As_{30}S_{70}$ films // *Solid State Ionics*, **141–142**, p. 387-395 (2001).
8. A. Kovalskiy, H. Jain, M. Mitkova, Evolution of chemical structure during silver photodiffusion into chalcogenide glass thin films // *J. Non-Cryst. Solids*, **355**, p. 1924-1929 (2009).
9. I.P. Studenyak, Yu.Yu. Neimet, Y.Y. Rati, D. Stanko, M. Kranjčec, S. Kökényesi, L. Daróci, R. Bohdan, Structural and optical properties of annealed and illuminated $(Ag_3AsS_3)_{0.6}(As_2S_3)_{0.4}$ thin films // *Opt. Mat.* **37**, p. 718-723 (2014).
10. I.P. Studenyak, Yu.Yu. Neimet, Y.Y. Rati, M.Yu. Buchuk, S. Kökényesi, L. Daróci, R. Bohdan, Structural and optical studies of $(Ag_3AsS_3)_{0.6}(As_2S_3)_{0.4}$ thin films deposited at different technological conditions // *Semiconductor Physics, Quantum Electronics & Optoelectronics*, **17**, p. 232-236 (2014).
11. I.P. Studenyak, M.M. Kutsyk, M.Yu. Buchuk, Y.Y. Rati, Yu.Yu. Neimet, V.Yu. Izai, S. Kökényesi, P. Nemec, Temperature studies of optical parameters of $(Ag_3AsS_3)_{0.6}(As_2S_3)_{0.4}$ thin films prepared by rapid thermal evaporation and pulse laser deposition // *Opt. Mat.* **52**, p. 224-229 (2016).
12. Yu.Yu. Neimet, I.P. Studenyak, M.Yu. Buchuk, R. Bohdan, S. Kökényesi, L. Daróci, P. Nemec, Photo-induced effects in $(Ag_3AsS_3)_{0.6}(As_2S_3)_{0.4}$ thin films and multilayers with gold nanoparticles // *Semiconductor Physics, Quantum Electronics & Optoelectronics*, **18**, p. 385-390 (2015).
13. R. Swanepoel, Determination of the thickness and optical constants of amorphous silicon // *J. Phys. E: Sci. Instrum*. **16**, p. 1214-1222 (1983).
14. F. Urbach, The long-wavelength edge of photographic sensitivity and of the electronic absorption of solids // *Phys. Rev*. **92**, p. 1324-1326 (1953).
15. H. Sumi, A. Sumi, The Urbach-Martienssen rule revisited // *J. Phys. Soc. Jpn*. **56**, p. 2211-2220 (1987).
16. M.V. Kurik, Urbach rule (Review) // *phys. status solidi* (*a*), **8**, p. 9-30 (1971).
17. M. Beaudoin, A.J.G. DeVries, S.R. Johnson, H. Laman, T. Tiedje, Optical absorption edge of semi-insulating GaAs and InP at high temperatures // *Appl. Phys. Lett.* **70**, p. 3540-3542 (1997).
18. Z. Yang, K.P. Homewood, M.S. Finney, M.A. Harry, K.J. Reeson, Optical absorption study of ion beam synthesised polycrystalline semiconducting $FeSi_2$ // *J. Appl. Phys.* **78**, p. 1958-1963 (1995).
19. G.D. Cody, T. Tiedje, B. Abeles, B. Brooks, Y. Goldstein, Disorder and the optical-absorption edge of hydrogenated amorphous silicon // *Phys. Rev. Lett*. **47**, p. 1480-1483 (1981).
20. I.P. Studenyak, M.M. Kranjčec, Gy.Sh. Kovacs, I.D. Desnica, V.V. Panko, V.Yu. Slivka, Influence of compositional disorder on optical absorption processes in $Cu_6P(S_{1-x}Se_x)_5I$ crystals // *J. Mat. Res.* **16**, p. 1600-1608 (2001).